ISBN: 978-3-95450-262-2 ISSN: 2673-5350 doi: 10.18429/JACoW-IBIC2025-MOBC01

MEASUREMENT OF NANOAMPERE BEAM INTENSITIES AT FAIR*

T. Sieber†, H. Braeuning, M. Schwickert, GSI, Darmstadt, Germany
L. Crescimbeni[1], Friedrich-Schiller-University Jena, Jena, Germany
T. Stoehlker[1,2], V. Tympel[1], Helmholtz Institute Jena, Jena, Germany
R. Stolz[3], V. Zakosarenko[4], Leibniz IPHT, Jena, Germany
G. Khatri, T. Koettig, J. Tan, CERN, Geneva, Switzerland
S. Kolbe, B. Voss, Ernst Abbe Hochschule, Jena, Germany
[1]also at GSI Helmholtz Centre for Heavy Ion Research, Darmstadt, Germany
[2]also at Institute for Optics and Quantum Electronics, Jena, Germany
[3]also at Technical University Ilmenau, Ilmenau, Germany
[4]also at supracon AG, Jena, Germany

Abstract

Analog to the working principle of standard beam transformers, the cryogenic current comparator (CCC) measures the intensity of particle beams via their azimuthal magnetic field. The superior performance of the CCC hereby derives from the high sensitivity of a SQUID (Superconducting Quantum Interference Device), which detects the current in the CCC pickup coil. This enables for a current resolution in the nA range, but in return needs extremely careful protection from external influences like stray fields and mechanical vibrations. The CCC therefore requires an elaborated superconducting magnetic shielding and is housed in a specially developed, vibration damped He bath cryostat.

We have recently achieved half a year of non-stop operation in stand-alone (closed Helium circuit) mode. The nA resolution has been demonstrated during several beamtimes, in CRYRING as well as with slow extracted beams from SIS18. Among the CCC types, which have been investigated, the 'Dual Core' (DCCC) version showed the best performance with respect to bandwidth and current resolution. The DCCC and its cryostat therefore mark a provisional closure of CCC development for FAIR.

In this contribution we present the latest results and the system status.

INTRODUCTION

During the last ten years, the CCC went through a process of steady optimization and redesigning to match the requirements in the storage rings and extraction lines at GSI/FAIR as well as in the CERN AD. The first prototype at GSI (1995) proved the possibility of nA intensity measurement by a CCC in an accelerator environment and was the groundbreaking idea and basis for all later work [1]. Looking back (and facing today's requirements at FAIR), this prototype had a number of severe disadvantages, which made it unsuitable for practical and longterm operation in the HEBT and excluded the operation in storage rings. The necessary development work to match the FAIR requirements covered the full spectrum of cryogenic, vacuum, mechanical properties, as well as external field attenuation, SQUID-electronics, DAQ and signal processing. Investigations performed by a collaboration of institutes specialized on the various subtopics resulted in a variety of CCC types with respect to field-pickup, magnetic shielding, SQUID types and SQUID coupling. Many of them have been tested under laboratory and under beamline conditions, which in total formed a detailed picture of the application possibilities for CCCs in accelerators. The details of this work are described in [2-4]. Latest achievements were spill measurements with a 'classical' radial Niobium CCC as well as with a Pb Dual Core DCCC at GSI SIS18, advanced filtering of periodic disturbance and - last not least - the stand-alone operation of the He bath cryostat for >6 months.

Regarding its basic principle the CCC consists of a superconducting magnetic shielding in combination with a pickup coil, which is connected to a SQUID. The shielding provides an attenuation of non-azimuthal external fields in the range -70 dB to -150 dB (depending on shield geometry). It guides the superconducting Meissner-Current to an internal pickup loop, which is basically a one-winding coil around a high permeability ring core as flux concentrator. The ring core is used in the 'classical' CCC, as shown in Fig. 1, to provide an efficient coupling of the beam magnetic field to the SQUID circuit. In later versions it was omitted (coreless CCC) or replaced by a pair of cores (DCCC).

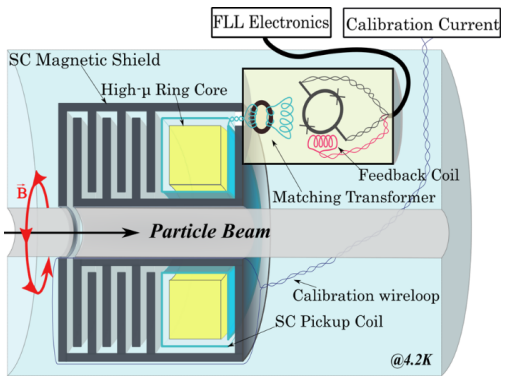


Figure 1: Classical CCC originally developed at the PTB (Physikalisch-Technische Bundesanstalt) [5].

*Supported by BMBF under contracts 05P18RDRB1 and 05P18SJRB1.
†T.Sieber@gsi.de

Content from this work may be used under the terms of the CC BY 4.0 licence (© 2025). Any distribution of this work must maintain attribution to the author(s), title of the work, publisher, and DOI.

ISBN: 978-3-95450-262-2 ISSN: 2673-5350 doi: 10.18429/JACoW-IBIC2025-MOBC01

Content from this work may be used under the terms of the CC BY 4.0 licence (© 2025). Any distribution of this work must maintain attribution to the author(s), title of the work, publisher, and DOI.

The arrangement is (like in an ACCT) basically a transformer with the particle beam as primary winding and the pickup coil as the secondary winding. The signal from the pickup coil is fed via an impedance matching transformer to the DC SQUID current sensor. A second coil is added to apply a calibration current.

On the electronics side, the SQUID is operated in a compensation circuit, using a so-called Flux Locked Loop (FLL) electronics, which provides via a feedback system a compensation of the magnetic flux induced by the pickup circuit (see Fig. 2, left). If the working point of the FLL system is locked to the steepest slope of the flux/voltage curve of the SQUID (see Fig. 2, right), the resolution can be in the order of $\mu\Phi_0$ (Φ_0 = magnetic flux quantum).

The current resolution of the CCC is therefore very much dependent on the stability of the SQUID flux/voltage curve. Another important aspect of the system is its slew rate limitation (min. rise time at a given current), which derives primarily from limited speed of the compensation circuit but is also strongly dependent on background noise and eigenfrequencies of the cold part of the CCC. Figure 2 shows schematically the FLL electronics and the corresponding voltage curve. For a more detailed description see for example [2].

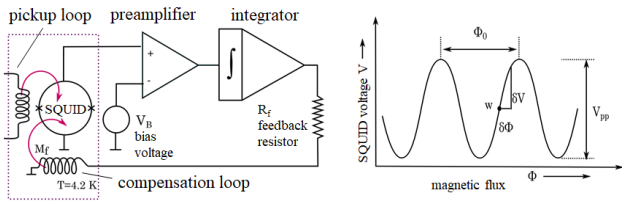


Figure 2: Left: schematic of the FLL electronics. Right: SQUID characteristic flux/voltage curve, W marks the working point. The Oscillation period is one flux quantum $\Phi_0 = h/2e = 2.06\times10^{-15}$ Tm^2.

AXIAL SHIELDING GEOMETRY

In the course of CCC optimization and redesigning it was proposed to build a CCC without toroidal core, using a shielding with axial meander geometry [6], consequently the device is called ‘coreless’ or ‘axial’ CCC. This shielding/pickup design provided - first in the simulations, later in laboratory measurements - a several orders of magnitude higher attenuation of external magnetic disturbances than the radial design, due to the increased meander path length and usage of thin lead foils. Manufacturing of the axial CCC turned out to be much easier than in the radial case (soldering instead of electron beam welding) and the shielding body has an inherent better mechanical stability, which significantly reduces weight. As a consequence, the axial geometry allows for lead as shielding material (instead of niobium), which reduces the costs by at least a factor 5.

The coreless axial CCC prototype could not be successfully operated in the FAIR cryostat due to its sensitivity to external noise and in general its weak coupling to beam (resp. calibration-) current [7], moreover, the expected improvements in noise sensitivity could not be verified. Based on these results a third CCC type, which combines the axial meander geometry with a doubled classical toroidal core pickup was developed [8], which achieved - besides excellent magnetic shielding - a current resolution equal or better than the classical, radial CCC. This version is called the ‘dual core’ or DCCC. Figure 3 shows the three mentioned varieties at one glance.

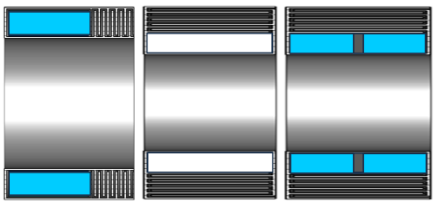


Figure 3: CCC magnetic shielding types: ‘classical’ radial meanders (left, like Fig. 1), axial meanders without ring core (middle) and axial meanders with dual ring core (right).

Figure 4 shows the noise figures of an axial CCC prototype, the ‘classical’ FAIR CCC and the old GSI prototype from the 90s. Obviously the FAIR CCC has the best performance, despite its large dimensions (inner/outer diameter: 250 mm/350 mm). The axial version with identical size shows almost one order of magnitude higher noise, even at very low frequencies, where an advantage due to the missing Barkhausen noise was expected. The old GSI CCC behaves still better than the axial version, mainly because of its small dimensions (inner/outer diameter: 150 mm/250 mm).

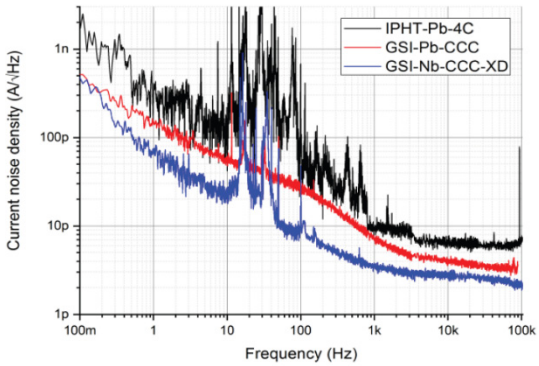


Figure 4: Noise spectra measured at the FAIR CCC-XD (blue), the GSI prototype from [1] (red) and one of the first prototypes of the axial CCC (black).

FAIR CCC-XD STORAGE RING OPERATION

The CCC-XD, a classical CCC version, in combination with its specially designed cryostat [9], was originally considered to be the first of series of five planned CCC systems at FAIR. Nonetheless, already during its construction and assembly, investigations on the coreless axial CCC started in parallel, with the goal to eliminate unwanted effects (low frequency Barkhausen noise, temperature dependent offset drift, microphony) related to the toroidal core. Additionally, a more efficient magnetic shielding to suppress the disturbing influence of nearby

ISBN: 978-3-95450-262-2 ISSN: 2673-5350 doi: 10.18429/JACoW-IBIC2025-MOBC01

dipole magnets seemed desirable as well as a higher slew rate to cope with fast pulses. Despite its drawbacks, the prototype of the CCC-XD was tested successfully in CRYRING@ESR, showing with appropriate filtering of dipole and cryostat effects with a current resolution <10 nA at 10 kHz bandwidth. Slew rate problems at higher currents and fast rise-times could be solved by damping the SQUID circuit with an inductive load. Figure 5 shows such a 'high current' measurement in CRYRING in comparison to standard diagnostics, IPM and DCCT (Bergoz PCT).

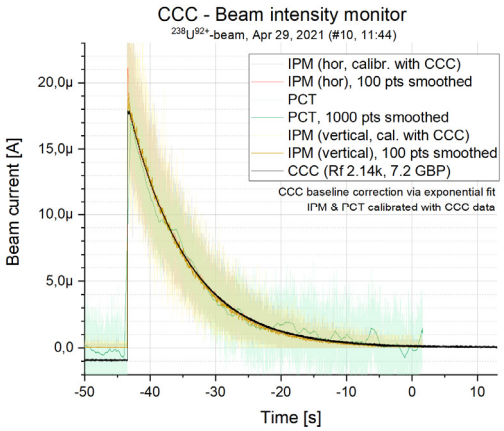


Figure 5: CCC current measurement compared to IPM and PCT in CRYRING. Rf = Feedback resistor value, GBP = Gain Bandwidth Product of the SQUID electronics [10].

While the results of the CCC-XD operation in CRYRING were promising and not too far from the current resolution achieved in the laboratory [3], a significant reduction of the SQUID performance was observed when moving to the accelerator environment. More specifically, the modulation swing of the SQUID voltage in the flux to voltage characteristics (see again Fig. 2) was reduced. Most likely the effect derived from ring-rf interference that reaches the detector through the enclosed beam tube. It could not be observed in transport sections or in the laboratory.

In addition to the reduced V/Φcurve the critical current of the SQUID was reduced by up to 70 %, which implies that the superconductor experienced additional strain imposed by the environment. We concluded that the presence of static or dynamic magnetic fields during cooldown were responsible for this effect.

The main perturbation of the system is created by the periodic He compression and expansion inside the attached pulse tube cryocooler (re-liquefier) at a fixed frequency of 1.4 Hz. Measurements with an accelerometer have shown that mechanical vibrations are strongly attenuated before they reach the cryostat, due to several measures taken for mechanical decoupling, however, there is evidence that the coupling is mainly based on the pressure fluctuations created by the periodic temperature variations at the cryocooler heat exchangers and its dimensional changes during the working cycle. While the frequency is stable, the phase of the cryo-cooler is fluctuating and the exact shape of the resulting signal at the CCC depends on the system state (e.g. remaining liquid helium level). This makes it difficult to use background measurements to directly subtract the 1.4 Hz noise source. Consequently, a digital FFT-based band-block filter was used to eliminate signals with a frequency between 1 and 3 Hz. The effect of this filtering can be seen in Fig. 6.

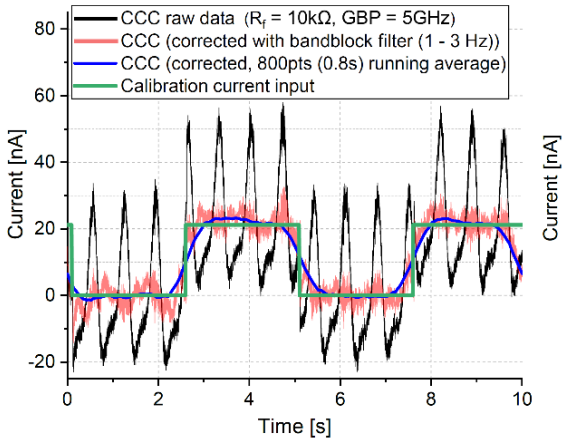


Figure 6: Effect of the liquefier on the current signal, periodic disturbance at 1.4 Hz and filtering / averaging.

Concerning magnetic disturbances, it was found that despite the strong field attenuation by the superconducting shield a stray field from the neighboring dipoles reached the CCC and produced a signal with a maximum amplitude of ~23 nA, following the dipole ramp (see Fig. 7). Since the ramp of the dipole is deterministic, the response of the CCC can be measured beforehand and then be subtracted from the beam. The blue line in Fig. 7 shows the CCC signal during a background measurement after the elimination of the dipole using the recorded data.

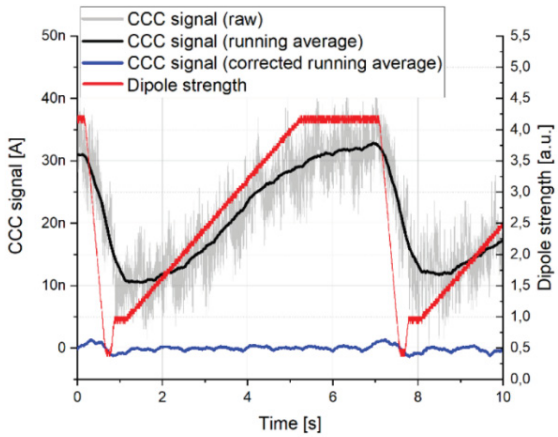


Figure 7: Effect of dipole ramp in CRYRING on CCC-XD measurement.

An important advantage while measuring in storage rings is the possibility of averaging at beam lifetimes of several seconds. Figure 8 shows a measurement at the lower end of the detection range. Dipole correction and bandblock filtering have been applied, the advantage of averaging is evident and underlines the challenge of measurements with single pass beams in HEBT, where averaging would remove the information about individual spill structure.

Content from this work may be used under the terms of the CC BY 4.0 licence (© 2025). Any distribution of this work must maintain attribution to the author(s), title of the work, publisher, and DOI.

ISBN: 978-3-95450-262-2 ISSN: 2673-5350 doi: 10.18429/JACoW-IBIC2025-MOBC01

Content from this work may be used under the terms of the CC BY 4.0 licence (© 2025). Any distribution of this work must maintain attribution to the author(s), title of the work, publisher, and DOI.

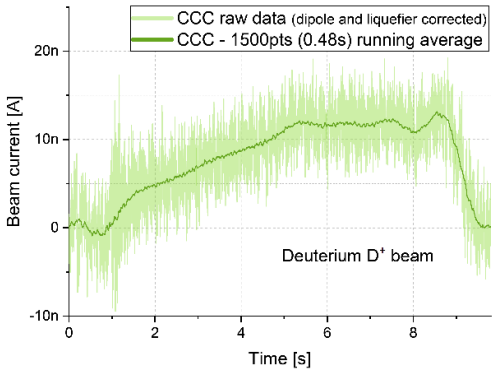


Figure 8: Stored low intensity $^2D^+$ beam in CRYRING.

DCCC SPILL MEASUREMENTS

Figure 9 shows the comparison of current noise densities of the coreless axial CCC and the DCCC (to be compared with Fig. 4). The DCCC noise is on average one order of magnitude lower, similar to the FAIR CCC-XD, whereby the dual core concept even allows for subtraction of the (180° inverted) signals from the two SQUIDs, which further improves the SNR. To enhance the dynamic range, one of the two cores (pickups) is equipped with an additional, less sensitive SQUID, so it can measure up to ~10 µA range.

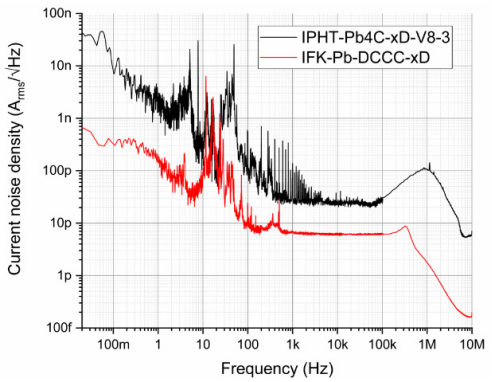


Figure 9: Comparison of current noise from an axial CCC prototype (black) and a DCCC (red), both with outer diameter: 350 mm.

An advanced prototype of the DCCC was installed in an experimental cave at SIS18 synchrotron. In a first campaign we used a 400 MeV/u Erbium 57+ beam with ~5*10^8 particles per spill and later a 400 MeV/u Ar 18+ beam with ~2*10^9 particles. The spills had nominal lengths between 100 ms and 1 s. At low Erbium intensity short spills were used to reach usable intensities. By variation of the extraction times, the nA measurement could be demonstrated, moreover the DCCC could be used for analysis of the spill quality and showed the potential as a detector for an automatic spill optimization system, which was developed at GSI [11], the latter with some limitation because of slew rate problems and bad spill quality. Figure 10 shows an example for the so called "tune wobbling" technique [12], which is applied to quadrupole driven extraction. A periodic signal is superimposed to the control voltage of the quadrupole, which drives the particles to betatron resonance. Due to the "wobbling" the effect of the power supply noise is reduced, which results in a more homogeneous spill structure and therefore higher detector efficiency at physics experiments.

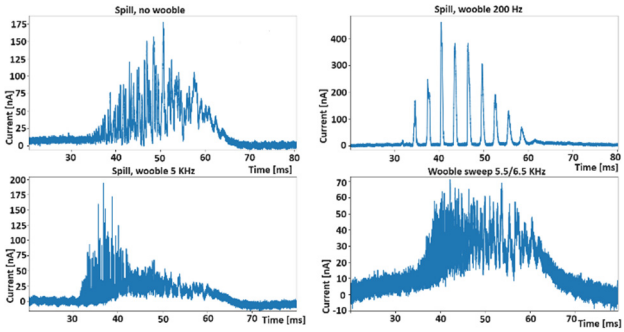


Figure 10: 30 ms spill (5*10^8 Ar 18+ per spill). Top left: uncorrected spill. Top right: 200 Hz wobbling frequency, spill modulation. Bottom left: 5 kHz, spill starts to smoothen out (frequency higher than beam cutoff frequency, around 4 kHz). Bottom right: Optimal setting for spill quality (6 kHz Δf = 500 Hz).

The DCCC showed a much higher bandwidth than the CCC-xD (200 kHz compared to 11 kHz) and is at the same time more stable towards fast current changes (slew rate DCCC = 0.4 µA/µs; slew rate CCC-xD = 0.16 µA/µs). The reason for this behavior lies in the resonant properties of the composite detector system (shielding, pickup, matching and SQUID). Figure 11 shows the resonances of the two systems, which are in both cases around 200 kHz. This kind if resonance obviously would make FLL operation impossible, so it needs to be suppressed. Figure 11 illustrates that this suppression/damping results in a much higher cut off frequencies for the DCCC, which again increases its slew rate.

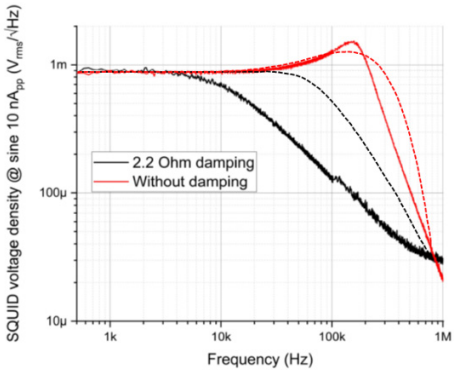


Figure 11: Effect of resonance damping and cut off frequencies in the CCC-xD (measured, solid) and the axial DCCC (calculated, dotted). The increased noise floor due to the damping resistor (2.2 Ohm) is visible in the CCC-xD curves.

Concerning mechanical disturbances, Fig. 12 shows the noise contributions in the range 1 to 100 Hz. As said before, the main source of periodic mechanical noise is the 1.4 Hz oscillation from the liquefier and harmonics. Other noise

ISBN: 978-3-95450-262-2 ISSN: 2673-5350 doi: 10.18429/JACoW-IBIC2025-MOBC01

contributions are pumps as well as mechanical eigenmodes of the cryostat itself. Since the ramping/slow extraction process is in the order of seconds, the data can digitally be filtered offline by simple subtraction of the disturbing frequencies from the FFT spectra. The spill measurement appears in real-time, while the filtered result can even be used as feedback for spill optimization schemes.

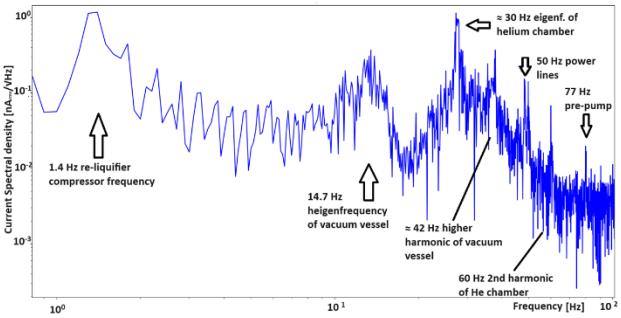


Figure 12: Mechanical noise sources in the range below 100 Hz with strong sources identified.

As an example, Fig. 13 shows a measurement of an U^{28+} 300 ms spill at a current of ~30 nA with and without software filtering. A (software) narrow band-pass filter at 1.4 Hz, 2.8 Hz and 4.2 Hz removes the most prominent noise components while keeping the particle number accurate within 1 %. The general noise floor was around 5 nA. More sophisticated filtering approaches are currently under development. The strategy is to use the differences between the noise signals of the two SQUIDs to enable algorithmic suppression, based on summation, correlation analysis or adaptive filtering (with one channel as a reference for the noise signal). Phase based filtering (using the exact 180° shift of the beam signals) is under discussion.

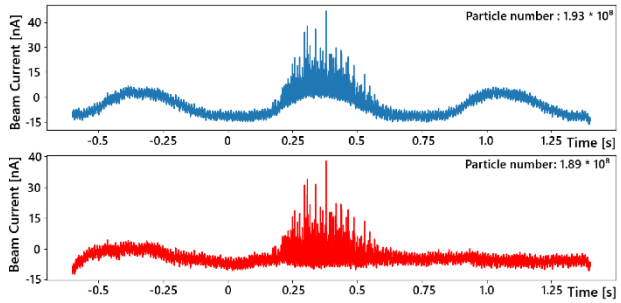


Figure 13: Raw (top) and filtered (bottom) U^{28+} spill.

CRYOSTAT STAND ALONE OPERATION

A dedicated He bath cryostat has been designed, which fulfils the requirements of maximum stability and homogeneous cooling, UHV suitability, nonmagnetic material, vibrational damping, short insertion length and accessibility for maintenance and repair work. The outer dimensions of the isolation vacuum vessel are 1.2 m x 0.8 m x 0.8 m. It consists of a stainless-steel frame, covered by aluminum windows, which enable for access to all inner components. Figure 14 shows a 3D model.

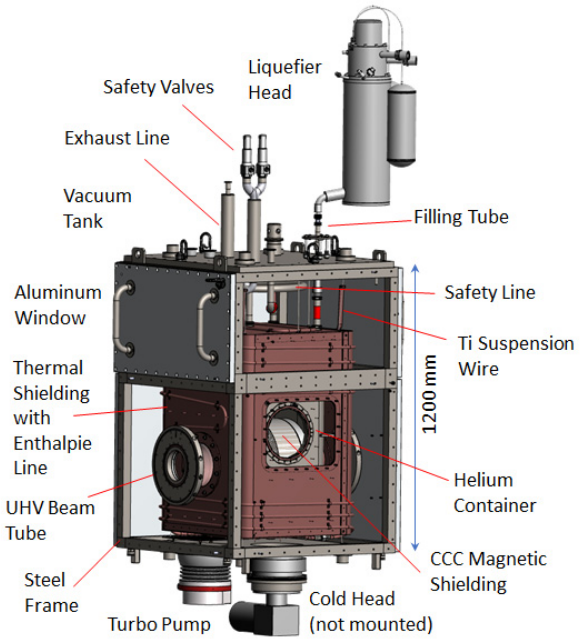


Figure 14: FAIR CCC cryostat with Cryomech© HeRL25 liquefier.

A complex system for gas handling and re-liquefaction has been worked out to achieve completely autonomous operation, which is necessary in FAIR tunnels without cryogenics infrastructure. We started the latest test campaign in Nov 24 and finally ran out of helium mid May 25. The 'gas mode' operation at 6 to 7 K would have been possible for some weeks more. The filling level at start was around 50 l. Although this is an encouraging result and sufficient for beamtime periods at FAIR, we want to avoid any intervention in the tunnels (except unavoidable maintenance), therefore further investigations are necessary to identify loss mechanisms in the He circuit. Nonetheless it could be demonstrated that our combination of cryostat and liquefier is suitable for long term stand-alone operation.

SUMMARY AND OUTLOOK

Because of its superior magnetic shielding, bandwidth and slew rate as well as its very good and upgradable noise behavior the DCCC is chosen as detector for FAIR. The lead construction reduces the costs for the device significantly (~1/5 of detector costs). Work is ongoing to improve the balance between the dual SQUIDs (-> noise suppression) and for filtering of periodic noise (liquefier, pumps, mech. eigenmodes). A simple approach with notch filters shows already good results, more sophisticated filtering will be implemented in the CCC FESA class.

Our cryostat in connection with a Cryomech liquefier has recently achieved 6 months of continuous operation, currently tests are performed to find the reason for the (even though small) He losses.

Content from this work may be used under the terms of the CC BY 4.0 licence (© 2025). Any distribution of this work must maintain attribution to the author(s), title of the work, publisher, and DOI.

ISBN: 978-3-95450-262-2 ISSN: 2673-5350 doi: 10.18429/JACoW-IBIC2025-MOBC01

© Content from this work may be used under the terms of the CC BY 4.0 licence (© 2025). Any distribution of this work must maintain attribution to the author(s), title of the work, publisher, and DOI.

REFERENCES

[1] A. Peters *et al*., "A Cryogenic Current Comparator for the absolute Measurement of nA Beams", *AIP Conf. Proc*., vol. 451, pp.163-180, 1998. doi:10.1063/1.56997

[2] F. Kurian, "Cryogenic Current Comparators for precise Ion Beam Current Measurements", PhD thesis, University of Frankfurt, Frankfurt, Germany, 2015.

[3] D. Haider, "Precise intensity monitoring at CRYRING@ESR: On designing a Cryogenic Current Comparator for FAIR", PhD thesis, University of Frankfurt, Frankfurt, Germany, 2022.

[4] L. Crescimbeni, "Development of the axial Cryogenic Current Comparator for FAIR", PhD thesis, University of Frankfurt, Frankfurt, Germany, 2025 (in preparation).

[5] K. Grohmann, H. D. Hahlbohm, D. Hechtfischer, and H. Lübbig, "Field attenuation as the underlying principle of cryocurrent comparators 2. Ring cavity elements", *Cryogenics,* vol. 16, no. 7, pp. 423-429, 1976. doi:10.1016/0011-2275(76)90056-4

[6] V. Zakosarenko *et al.,* "Coreless SQUID-based cryogenic current comparator for non-destructive intensity diagnostics of charged particle beams", *Supercond. Sci. Technol.,* vol. 32, p. 014002, 2018. doi:10.1088/1361-6668/aaf206

[7] L. Crescimbeni *et al*., "Axial Cryogenic Current Comparator (CCC) for FAIR", in *Proc. IBIC'23*, Saskatoon, Canada, Sep. 2023, pp. 259-262. doi: 10.18429/JACoW-IBIC2023-TUP034

[8] M. Stapelfeld, "Experimentelle Untersuchungen zum Systemdesign von Kryogenen Stromkomparatoren'', PhD thesis Friedrich Schiller University Jena, Jena, Germany, 2022.

[9] T. Sieber *et al*., "Optimization Studies for an Advanced Cryogenic Current Comparator (CCC) System for FAIR", in *Proc. IBIC'16*, Barcelona, Spain, Sep. 2016, pp. 715-718. doi:10.18429/JACoW-IBIC2016-WEPG40

[10] Magnicon, http://www.magnicon.com

[11] P. J. Niedermayer, R. Singh, and R. Geißler, "Software-Defined Radio Based Feedback System for Beam Spill Control in Particle Accelerators", in *Proc. GRCon23*, 2023, Tempe, Arizona, USA, https://pubs.gnuradio.org/index.php/grcon/ article/view/133

[12] R. Singh, P. Forck, and S. Sorge, "Reducing Fluctuations in Slow-Extraction Beam Spill Using Transit-Time-Dependent Tune Modulation," *Phys. Rev. Appl*., vol. 13, no. 4, Apr. 2020. doi:10.1103/physrevapplied.13.044076